Available online at www.sciencedirect.com
ScienceDirect
Advances in Space Research 41 (2008) 936–942
ADVANCES IN SPACE RESEARCH (a COSPAR publication)
www.elsevier.com/locate/asr

On bandwidth of solar subsecond bursts in cm-range

N.S. Meshalkina [a,*], A.T. Altyntsev [a], Yihua Yan [b]

[a] Radioastrophysical Department, Institute of Solar-Terrestrial Physics, Lermontov St. 126, P.O. Box 4026, Irkutsk 664033, Russian Federation
[b] National Astronomical Observatories, Chinese Academy of Sciences, Datun Road A20, Chaoyang District, Beijing 100012, China

Received 2 August 2006; received in revised form 24 April 2007; accepted 25 April 2007

Abstract

The goal is to study parameters of drifting type III bursts, and find out the emission mechanism of these bursts and understand what factors affect instantaneous spectral bandwidth of these bursts.

We used simultaneous observations of microwave type III bursts with high temporal, spatial and spectral resolution from the Siberian Solar Radio Telescope (5.7 GHz, 14 ms resolution) and from the spectropolarimeters (5.2–7.6 GHz, 5 ms) of the National Astronomical Observatories.

Characteristic parameters such as starting frequency, total and instantaneous bandwidth, polarization degree, total duration, and rate of frequency drift were determined for the radio bursts. We analyzed and estimated parameters, which determine instantaneous bandwidth.

Keywords: Solar flares; Microwave emission; Bandwidth of spectrum

1. Introduction

The fine temporal structure takes up a special place among the different types of flare emission. This structure was revealed at individual frequencies as intense pulses lasting less than one second, which were superposed on broadband continuum emission of much longer duration. Their short duration implies a compact size of the emission source. Broadband spectrometer observations have shown that the fine temporal structure has different spectral features. The main structures are broadband pulsations, spikes, and bursts with frequency drift (Benz, 1986).

Spikes and drifting bursts have relatively narrow instantaneous frequency band of emission. Their emission can be coherent and excited by non-thermal electrons. The frequency drift is naturally explained by an emission source moving along the plasma density or magnetic field gradients. The frequency drift events can be confidently subdivided into two classes in the metric and decimetric range: bursts of types II and III, which differ in drift rates. We are justified to state that the type III bursts are related to accelerated electrons moving at velocities of more than 4×10^4 km/s, and the type II bursts are a reflection of shock wave fronts moving at magnetosonic velocities (200–2000 km/s).

In the centimetric range (4–8 GHz) these structures were first classed in a study by Allaart et al. (1990). It was revealed that the centimetric range is peculiar in that the frequency drift is predominantly towards higher frequencies as well as exhibiting a wide range of absolute values of drift rates, 0–20 GHz/s. Two groups of frequency drifting structures were singled out, with drift rates above/below 2 GHz/s. These groups differ from each other in intensity and duration. As shown in Bruggmann et al. (1990), the direction of the drift in the centimetric range is observed to be towards higher frequencies, with a mean rate of about 4 GHz/s and scatter of the order of the mean value. Benz et al. (1992) explained the observable characteristics of the drifting bursts by plasma oscillations excited by an accelerated electron beam. It was suggested that electromagnetic

* Corresponding author. Tel.: +7 3952 511841; fax: +7 3952 511675.
E-mail address: nata@iszf.irk.ru (N.S. Meshalkina).

0273-1177/$30
doi:10.1016/j.asr.2007.04.074

emission is generated when longitudinal plasma oscillations merge, i.e. the drifting bursts were regarded as type III bursts emitted by electron beams. Absorption of electromagnetic emission by the background plasma is large as distinct from the low-frequency type III bursts. In this case, it is necessary to assume that the emission is in a transverse direction from thin magnetic filaments ($\sim$100 km) with high plasma density ($\sim 10^{11}$ cm^{-3}).

A new stage in the research into the drifting bursts in the centimetric range began when the possibility appeared to simultaneously observe the burst spectrum and distributions of radio brightness with the millisecond temporal resolution. Interferometric observations of the sources of fine temporal structure make it possible to localize them into flare loops and determine the temperature and plasma density in the source using soft X-ray images of the flare region. By now, analysis of such observations for some events with drifting bursts has been made (Altyntsev et al., 2003; Meshalkina et al., 2004, 2006). It was established that the emission frequency of drifting bursts corresponds to the doubled Langmuir frequency, the plasma temperature is typical for flare loops (about 10^7 K), the magnetic field value does not exceed 70–200 G.

The wide scatter of drifting burst parameters in the drift rate, the polarization degree, etc. point to the possibility of different generation mechanisms. Therefore, the study of statistic characteristics of drifting bursts is very relevant. The characteristics of a large number of bursts were analyzed by Ning et al. (2005). Twenty-two groups of drifting bursts during 1999–2003 have been revealed with the Purple Mountain Observatory (China, 4.5–7.5 GHz). Data for the mean drift rate in the group, and for the number and repetition frequency of drifting bursts during one flare event were analyzed in that paper. As in previous studies, the frequency drift rate varied over a wide range with the mean value of about 7 GHz/s.

The primary drift towards higher frequencies and the large scatter of drift rates may be explained by acceleration of electron beams near the tops of closed flare loops in terms of the type III burst conception. This assumption was confirmed for some bursts in Meshalkina et al. (2004). When moving down in the denser plasma region, accelerated electron beams excite Langmuir oscillations with frequency increasing with time. This is due to preferential downward propagation into denser plasma layers of accelerated electron generating Langmuir oscillations with frequency increasing with time.

Analysis of statistic characteristics of instantaneous spectral bandwidths of drifting bursts is very important for determining their generation mechanism. At the centimetric range, an analysis of such data was made for narrowband driftless subsecond pulses, which are known as spikes. Csillaghy and Benz (1993) have showed that the range of bandwidths was relatively large. It has been found that the spectral bandwidth displays very large scatter both inside one event and from one burst to another and individual bandwidths show a scatter of a factor 2–3 or more within an event. The minimal relative bandwidth was about 0.65% for spikes. It was assumed that the observed instantaneous spectral bandwidth is determined by inhomogeneity of plasma parameters (density and magnetic field) across the source. In that case changes in the spike bandwidth are naturally explained by changing emission source sizes.

Nowadays, instruments which measure positions of subsecond structure microwave sources simultaneously with the dynamic spectrum of their radio emission are the solar radio spectrometers in China [Solar Radio Broadband Fast Dynamic Spectrometers (SRS) and Purple Mountain Observatory (PMO)] and the Siberian Solar Radio Telescope (SSRT) in Badary of the Buryat Republic (Russian Federation). This paper is concerned with description of the measuring methods of drifting burst parameters, as well as with statistical analysis of their parameters. For the analysis, we use bursts simultaneously registered at the SRS (5.2–7.6 GHz) in Huairou (Beijing) and by the Siberian Solar Radio Telescope (SSRT, 5.7 GHz) for 2000–2004. The simultaneous independent observations from both instruments give us an assurance these events have solar origin. In this case, particular attention has been given to research into spectral characteristics of drifting bursts.

2. Observation

For the analysis we have selected events with subsecond pulses using the entire data set (183 events with fine temporal structure), recorded with the SSRT at 5.7 GHz for the period 2000–2004 (http://badary.iszf.irk.ru/Ftevents.php and http://ssrt.iszf.irk.ru/fast/). The Siberian Solar Radio Telescope (SSRT) is a crossed radio interferometer, operating in the frequency range 5.67–5.79 GHz (Smolkov et al., 1986; Grechnev et al., 2003). The components of circular polarization (R and L) are recorded alternately for an interval of 7 ms each.

The SSRT data were used to determine coordinates of the fine temporal structure sources on the solar disk. Dynamic spectra were observed with the Solar Radio Broadband Fast Dynamic Spectrometers (5.2–7.6 GHz frequency range, 120 frequency channels) at Huairou Solar Observing Station of the Beijing Astronomical Observatory (Fu et al., 1995). The receiving band of a single frequency channel of the SRS spectropolarimeter is 20 MHz, and the temporal resolution is 5 ms. The components of circular polarization (R and L) were recorded simultaneously. For the SSRT data set the dynamic spectra of SRS were available for 114 events. Among them we have found 21 events with well-distinguishable drifting structures (see, e.g. Fig. 1). Total number of such bursts was 136 (14 with reverse drift) for these 21 events. During the event, several drifting bursts (from 2 to 12) have been observed except the flare on 30 March 2001, with 62 drifting bursts during 1 min.

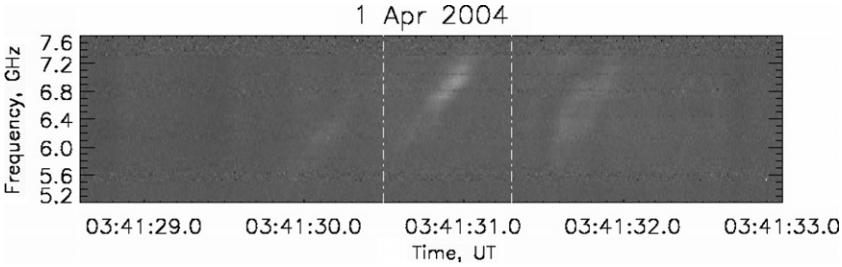

Fig. 1. A fragment of the dynamic spectrum with drifting bursts registered on 1 April 2004. The vertical lines indicate the burst interval, analyzed in Fig. 2.

Burst parameter measurement errors at SRS dynamic spectra are associated with signal fluctuations. That is why the drift rate and instantaneous bandwidth were evaluated using special procedures (see Fig. 2). The drift rate $\partial f/\partial t$ was calculated as a linear interpolation of cross-correlation maximum positions of frequency channel time profiles (by the method of least squares). The total width of Δf emission band was determined at the half-height of the frequency cross-correlation maximum distribution Fig. 2b.

To determine the instantaneous spectral width δf, these time profiles were sequentially displaced in time in order to compensate the frequency drift, and summarized with significant burst amplitude in the frequency range. As a result, the averaged time distribution of the burst radio brightness with δt width was found. The instantaneous spectral half-width of the drifting burst was calculated from the frequency drift width and rate thus: $\delta f = \delta t \cdot \frac{\partial f}{\partial t}$. For the event presented in Figs. 1 and 2, the drifting burst is observed in the frequency range 6.2–7.5 GHz. The drift rate is 5.3 GHz/s, and the instantaneous spectral width is about 0.5 GHz or 7% of the carrier frequency.

The histogram of drifting burst distributions according to drift rate is presented in Fig. 3. The absolute values of drift rates vary from 1.1 to 24.4 GHz/s. The drift rates scatter symmetrically around 7.3 GHz/s. The frequency drift rates of most bursts are positive, i.e. consistent with frequency increasing with time. The distribution displays an interval from 3 to 13 GHz/s (“bulk”, 99 events of 136 ones), outside which (“tail” bursts) event occurrence abruptly decreases. Fig. 4 shows burst duration distribution. The majority of the bursts lasted less than 0.2 s, with “tail” bursts generally shorter, their distribution maximum being shorter than 0.1 s.

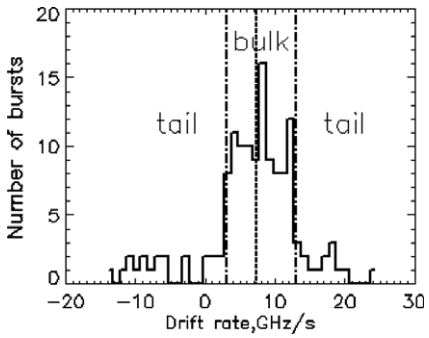

Fig. 3. The drifting burst distribution according to drift rates. The vertical dotted line shows the mean value 7.3 GHz/s.

Fig. 5 shows the bandwidth distributions for “bulk” and “tail” bursts corresponding to high drift rates. It can be

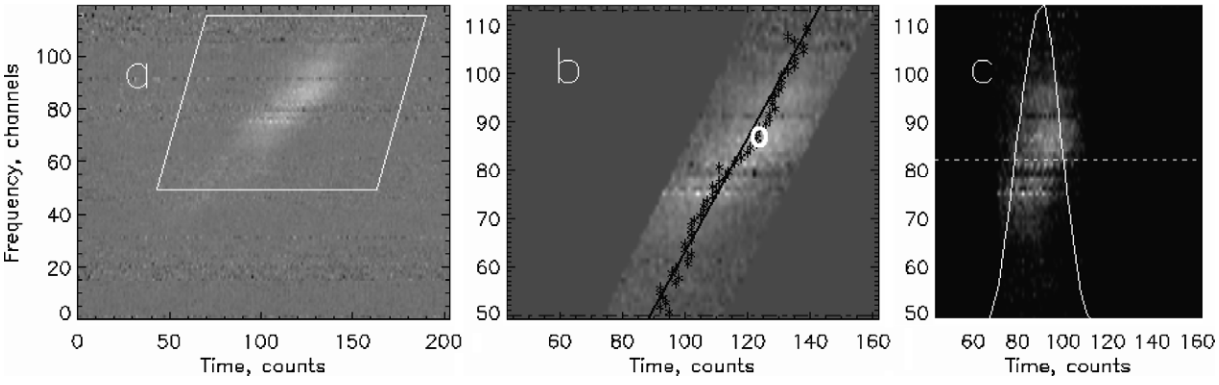

Fig. 2. Technique for determining drift rate and instantaneous bandwidth. (a) The parallelogram outlines the fragment with the burst. Frequency channel numbers and 5 ms time intervals are shown along the axes; (b) the same fragment. The white oval marks the center of the reference time profile. Black stars indicate maximum cross-correlations of different-frequency time profiles with the reference one. Horizontal black lines mark the frequency range, in which the burst flux is more than half the maximum value; (c) the result of a parallel shift of frequency channel time profiles within the (b) panel frequency range, compensating for the $\frac{\partial f}{\partial t}$ frequency drift calculated from the values on the b panel. The solid line shows an integral over the shifted time profiles. The horizontal line is half-height; the interval between vertical lines δt is equal to the width of radio brightness of a drifting burst righted about the frequency drift.

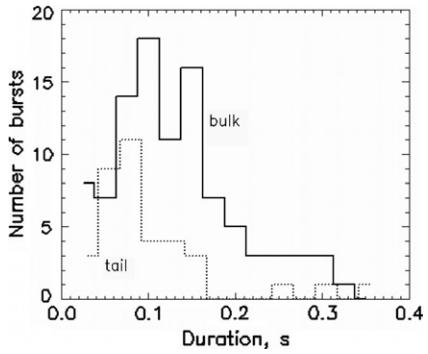

Fig. 4. The duration distribution of the bursts. The solid line represents the bursts with drift rates between 3 and 13 GHz/s; the dotted line represents the bursts with drift rates out of this rate interval.

seen that the instantaneous bandwidth values are comparable to the total width. The values of the instantaneous spectral bandwidth range from 0.1 to 2.6 GHz, and are mainly less than 1.5 GHz. The burst occurrence rate for the instantaneous bandwidth decreases faster with increasing emission bandwidth. This dependence retains its form, when we use a burst medium frequency-normalized width, instead of the instantaneous bandwidth value. The relative instantaneous bandwidth does not exceed 15% for 70% of the bursts.

Fig. 6 (bottom panel) displays the dependence of the relative instantaneous width of emission $\delta f/f$ on the drift rate. Let us note that minimum values do not exceed 3–4% in a wide range of drift rates from −10 to 10 GHz/s. With rising drift rate the spread of $\delta f/f$ values increases and the maximum value exceeds 40%.

The top panel shows the dependence of δf on the position of the burst source on the solar disk. A large number

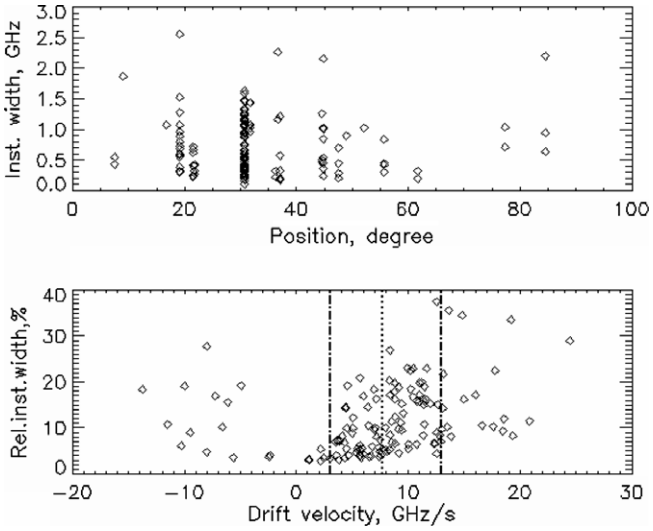

Fig. 6. Top: dependence of instantaneous spectral width on the angular distance of the source position from the solar disk center; bottom: dependence of relative instantaneous spectral width on values of the drift rates.

of bursts at 30° corresponded to the 30 March, 2001 flare, in which a large number of bursts were observed. On the whole, no statistically significant dependence of the instantaneous width upon the position on the disk is observed. Let us point out that flares with drifting bursts are unevenly distributed throughout the solar disk. The majority of such events (14 of 21 flares) were registered over the longitudinal range 15–45°, which shows emission anisotropy.

The degree of burst polarization varied in a wide range for both electron populations. The portion of bursts with polarization degree below 30% was about 75%. Note that

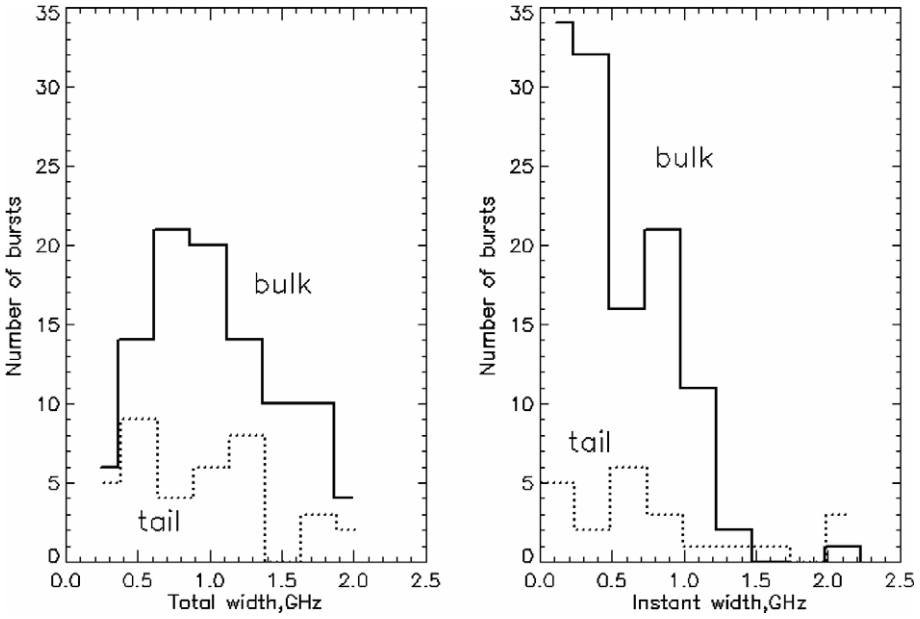

Fig. 5. The distribution of emission bandwidths of the drifting bursts. The solid line indicates all of the bursts; the dotted line – "tail" bursts. Left panel is for the total bandwidth Δf, right one – for the instantaneous width δf.

Table 1
The correlation coefficients between the some measured parameters

	Duration	Absolute drift velocity	Total bandwidth	Distance from solar disk center	$\Delta f/f_{mean}$	Polarization degree
Duration		−0.46	0.293	0.262	−0.097	−0.068
Absolute drift velocity			0.361	−0.227	0.460	−0.023
Total bandwidth				−0.101	0.523	−0.17
Distance from solar disk center					0.038	−0.076
$\Delta f/f_{mean}$						−0.005

the above dependences are similar for all events excepting 30 March, 2001 and separately for 30 March, 2001.

We have found correlation coefficients between the next measured parameters: burst duration, mean frequency, drift rate, total bandwidth, distance from solar disk center, polarization degree, ratio between instantaneous spectral width and mean frequency (Table 1).

Our analysis has shown that the largest correlation coefficient was 0.4603 (between drift rate and $\Delta f/f_{mean}$), for duration and absolute value of drift rate correlation coefficient was −0.4600.

3. Discussion

The analysis of the statistical characteristics of drifting bursts can briefly be summarized thus:

1. The distribution of bursts according to frequency drift rates is close to the symmetrical form relative to the mean drift value of about 7 GHz/s (the analysis was performed for all of the bursts except the bursts of the event on 30 March, 2001). Note that this conclusion is also correct for the event of 30 March, 2001, in which less than half of the analyzed bursts (namely, 62 of the total 136) were observed. The mean drift rate is close to the value obtained from PMO observation data (Ning et al., 2005).
2. The burst distribution pattern according to frequency drift rates justifies a subdivision of bursts into two groups. Bursts which rates ranging 3–13 GHz/s can be assigned to the first – main, ''bulk'' – group. Bursts with large absolute values are placed into the second, ''tail'', group.
3. The total burst duration is less than 0.5 s. The total width of drifting burst emission is generally less than 1.5 GHz, whereas the instantaneous width is less than 1 GHz. At the same time, the majority of the ''tail'' bursts are broadband.
4. The burst instantaneous band width is minimal, less than 3%, for low frequency drift rates. As drift rate increases, its values and scattering rise by an order of magnitude. No dependence was observed between the instantaneous width and the position on the disk.
5. The polarization degree of bursts, as a rule, does not exceed 30%, and no significant drift rate, disk position, or instantaneous spectral width dependences are observed.

When determining the generation mechanism, the first question that arises is whether the emission mechanism is coherent or incoherent. In this case pulse duration is not determinative because broadband subsecond pulses may be produced by the gyrosynchroton mechanism of non-thermal electron beams at the footpoints of flare loops (Altyntsev et al., 2000). A pulse-to-pulse correlation between the microwave and hard X-ray emission with photon energies of 25–50 keV is evident in these events.

As evident from the analysis, the bandwidth of gydrosynchron emission is bounded from below by $\geqslant 3$ GHz (Bruggmann et al., 1990; Giménez de Castro et al., 2006), which value can be realized in a source with high plasma density if the spectrum of emitting non-thermal electrons rapidly decreases with energy. The question of frequency drift nature remains open. In our case (Figs. 5 and 6), instantaneous emission bands are considerably narrower, which gives grounds to conclude that the mechanism of drifting burst emission is coherent. Abnormally, high brightness temperature of the source is generally perceived as a feature of the coherent mechanism. However, it can only be evaluated by indirect estimates of the source size, with already given emission mechanism and variation scales of background plasma parameters. At present there are no instruments to directly measure the brightness temperature of subsecond pulse sources with several arc sec sizes.

By now a number of events with drifting bursts have been analysed (Altyntsev et al., 2003, 2007; Meshalkina et al., 2004) using simultaneous observations at SSRT and SRS spectropolarimeters. The burst sources were demonstrated to be placed mainly in compact regions near flare loop tops, in which the magnetic field does not exceed $B = 100$–200 G, and the plasma density is $n \approx 10^{11}$ cm^{-3}.

Knowing plasma parameters in the source, we can compare frequencies of the narrowband observable emission with frequencies of free plasma oscillations. For these parameters, the electron cyclotron frequency is considerably less than plasma frequency and registered emission frequencies. Consequently, we can exclude the electron cyclotron maser as a generation mechanism of the fine spectral structure (e.g., Fleishman and Melnikov, 1998). With plasma density of 10^{11} cm^{-3}, the reception frequency (about 6 GHz) is close to the plasma frequency harmonic. For the fundamental frequency, plasma density in the source should be four times higher, which not only is less compatible with X-ray measurements, but results in

additional difficulties for the emission escaping from the source and explanation of low emission polarization. The most essential is fast emission absorption at the fundamental frequency in the plasma surrounding the source. With $T = 10$ MK and $H = 1000$ km, the optical depth is $\tau \approx 5$ for the fundamental emission and $\tau \approx 0.12$ for the second-harmonic emission. Thus, subsecond impulsive emission near the Langmuir frequency is suppressed (Bruggmann et al., 1990).

The instability responsible for the plasma wave amplification can be either a beam-like or loss cone instability. It is obvious that the observed spectral width consists of natural bandwidth (appearing in homogeneous source) and contribution of inhomogeneity of the real source.

For type III bursts beam-plasma instability is usually considered. For beam plasma instability our estimations showed that the minimal spectral bandwidth $\Delta f/f_{\text{mean}} = 3.1\%$. The "natural" bandwidth is determined as

$$\frac{\Delta f}{f} = \frac{T_0}{T_b}\frac{\Delta v_b}{v_b}, \tag{1}$$

where $T_0 = 10^6$–10^7 K is plasma temperature, T_b is beam temperature, v_b is beam velocity. In that case if $T_b \approx 3 \times 10^8$ K (30 keV) and $\Delta v_b/v_b \cong 0.33$ $\Delta f/f_{\text{mean}} \approx 1.1\%$, i.e. observed minimal spectral bandwidth is more than "natural".

Plasma oscillation excitation is due to non-thermal electrons with the nonequilibrium distribution function appearing in the source. The burst drift with frequency can be described as follows (Altyntsev et al., 2007):

$$\frac{df}{dt} = \frac{\omega_{pe}}{\pi n}\left(\frac{\partial n}{\partial t} + \frac{\partial n}{\partial l}v\right) \approx 6_{\text{GHz}}\left(\frac{V}{\Delta} + \frac{v_b}{L}\right). \tag{2}$$

The first term in parentheses governs the density change in time because of magnetohydrodynamic processes, the second term describing the displacement of emitting electron population along the plasma density gradient at velocity v. Here, V is the typical velocity of MHD motions resulting in plasma density increase in the source of size Δ across the magnetic field, v_b is the velocity of emitting electron motion along the density gradient, L is the typical scale of density change along the magnetic field. Eq. (2) accounts for the emission recorded at the doubled plasma frequency. With observable mean values $\frac{df}{dt}$, the expression in parentheses should be about 1 Hz.

Drift rate is usually interpreted without considering the first term. In that case the Langmuir turbulence is assumed to be excited by an accelerated electron beam along the magnetic field with electron beam distribution over longitudinal velocity component. Here the frequency drift rate is determined by the upper estimate of the total spectrum width of the drifting burst or by the path length of emitting electrons. Using the mean observable values $\frac{df}{dt} \approx 7$ GHz/s and $\Delta f = 1.5$ GHz, we can estimate the total path length of emitting electrons $\lambda_{\text{cm}} \sim 0.5L$. If the path length is determined by Coulomb collisions $\lambda_{\text{cm}} = 3.1 \cdot 10^{-20}(v_b^4/n)$, then from the condition $\frac{v_b}{L} \approx 1$ Hz we obtain an estimate for the emitting electron velocity $v_b \geqslant 10^{10}$ cm/s, corresponding to the energy of about 30 keV. This velocity value is close to estimates obtained when analyzing the observations in the decimetric range; and if the pulse duration is about 0.1 s, we estimate the plasma inhomogeneity scale within $L = 20{,}000$–$60{,}000$ km.

The upper estimate of the longitudinal size of the emission region Δx can be obtained using the instantaneous spectral width. If the instantaneous spectral width is determined by the background plasma density on the beam length, we can write $\frac{\delta f}{f} \approx \frac{\Delta x}{2L}$. As follows from the dependence in Fig. 6, we have a minimum value $\frac{\delta f}{f} = 0.03$, and thus $\Delta x = (1.2$–$3.6) \times 10^3$ km. On the other hand, we have $\delta f = \delta t \cdot \frac{\partial f}{\partial t}$, where duration at an isolated frequency can be estimated as $\delta t = \frac{\Delta x}{v_b}$. We observe $\Delta f/f_{\text{mean}}$ of up to 40% in some cases. Thus, the instantaneous spectral width should increase with increasing absolute frequency drift rate, and the value scattering may be associated with the scattering of longitudinal sizes of the acceleration region and emitting electron velocity.

It should be noted that we have previously analyzed the event of 30 March, 2001 (Altyntsev et al., 2007). Its distinctive peculiarity was the registration of subsecond pulse sources simultaneously on frequencies about 5.78 and 5.69 GHz (SSRT), which allowed us to make independent estimations of both the plasma density gradient along the source motion and exciter velocities. The measured drift rates were widespread around a nearly constant value of about 6 GHz/s. Electrons with a large velocity component across the loop (large pitch angles) had small displacements along the loop. The excess of large pitch angles implies that the electrons emitting subsecond drifting bursts are accelerated across the magnetic field, and Langmuir waves are excited by a loss cone driven instability. If so, then the observed drift rate of about 6 GHz/s cannot be attributed to the motion of beams along the density gradient, but should be considered as a response to a density increase in a site where the subsecond emission is generated. We have interpreted the observed distribution of the drift rates in terms of dynamic density increase in a region where the impulsive emission is generated.

Minimum spectral bandwidth for loss cone instability can be determined as:

$$\left(\frac{\Delta f}{f}\right)_{\text{min}} \cong \frac{1}{2}\frac{v_b^2}{c^2}\frac{\Delta\mu_c}{\mu_c}. \tag{3}$$

Simulation showed that the minimum spectral bandwidth of the emission mechanism $\Delta f/f = 0.01$ or 1% for reasonable parameters: accelerated particle energy $E_b = 30$ keV ($v_b/c \cong 0.33$), loss cone boundary $\mu_c = 30°$, loss cone boundary width $\Delta\mu_c = 15°$, plasma and magnetic field inhomogeneity scales 20,000 km (Kuznetsov, 2006).

Let us note that the dependences found by us (Table 1) are similar for all events except the event of 30 March, 2001 (74 bursts) and separately for 30 March, 2001 (64 bursts), indicating that spectral data alone cannot serve to

determine what type of instability (beam or loss cone) takes place in each particular case.

4. Conclusion

We have estimated the instantaneous spectral bandwidth of SSPs and studied the relationship between the bandwidth and position of the sources on the Sun and other emission parameters.

The drift rates scatter symmetrically around the mean drift value of about 7 GHz/s. The majority of bursts (72%) have drift rates 3–13 GHz/s.

The value of the instantaneous width of bursts is minimal with small frequency drift rates – under 3%. With increasing drift rate its magnitudes and scattering of values increase.

Several factors such as effects of source inhomogeneity and plasma density inhomogeneity along the propagation path of electron beam; longitudinal sizes of the acceleration region and emitting electron velocity, anisotropy of emission can influence the observed instantaneous spectral bandwidth.

Acknowledgments

This study was supported by Russian projects of RFBR No. 05-07-90147, 06-02-16295, 06-02-31004, 07-02-00101-a, and the Program of RAN No. 16.

References

Allaart, M.A.F., van Nieuwkoop, J., Slottje, C., Sondaar, L.H. Fine structure in solar microwave bursts. Solar Physics 130, 183–199, 1990.

Altyntsev, A.T., Nakajima, H., Takano, T., Rudenko, G.V. On the origin of subsecond pulses at 17 GHz. Solar Physics 195 (2), 401–420, 2000.

Altyntsev, A.T., Kuznetsov, A.A., Meshalkina, N.S., Yan, Y. On the origin of microwave type U-bursts. Astronomy and Astrophysics 411, 263–271, 2003.

Altyntsev, A.T., Grechnev, V.V., Meshalkina, N.S., Yan, Y. Microwave type III-like bursts as possible signatures of magnetic reconnection. Solar Physics, 2007.

Benz, A.O. Millisecond radio spikes. Solar Physics 104, 99–110, 1986.

Benz, A.O., Su, H., Magun, A., Stehling, W. Millisecond microwave spikes at 8 GHz during solar flares. Astronomy and Astrophysics Supplement Series 93, 539–544, 1992.

Bruggmann, G., Magun, A., Benz, A.O., Stehling, W. Solar flare microwave observations with high spectral resolution. Astronomy and Astrophysics 240, 506–510, 1990.

Csillaghy, A., Benz, A.O. The bandwidth of millisecond radio spikes in solar flares. Astronomy and Astrophysics 274, 487–496, 1993.

Fleishman, G.D., Melnikov, V.F. Solar millisecond radiospikes. Uspekhi Fiziologicheskikh Nauk 168, 1265–1301, 1998.

Fu, Q., Qin, Z., Ji, H., Pei, L. A broadband spectrometer for decimeter and microwave radio bursts. Solar Physics 160, 97–103, 1995.

Giménez de Castro, C.G., Costa, J.E.R., Silva, A.V.R., Simões, P.J.A., Correia, E., Magun, A. A very narrow gyrosynchrotron spectrum during a solar flare. Astronomy and Astrophysics 457 (2), 693–697, 2006.

Grechnev, V.V., Lesovoi, S.V., Smolkov, G.Y., et al. The Siberian Solar Radio Telescope: the current state of the instrument, observations, and data. Solar Physics 216, 239–272, 2003.

Kuznetsov, A.A. Generation of intermediate drift bursts by magnetohydrodynamic waves in the solar corona. Solar Physics 237, 153–171, 2006.

Meshalkina, N.S., Altyntsev, A.T., Sych, R.A., Chernov, G.P., Yan, Y. On the wave mode of subsecond pulses in the cm-range. Solar Physics 221, 85–99, 2004.

Meshalkina, N.S., Altyntsev, A.T., Grechnev, V.V., Yihua, Y. The signatures of magnetic reconnection according to the microwave drifting bursts observations, in: Solar Activity and its Magnetic Origin. Proceedings of IAU Symposium, 233, pp. 383–384, 2006.

Ning, Z., Ding, M.D., Wu, H.A., Xu, F.Y., Meng, X. Microwave type III bursts and pulsation groups. Astronomy and Astrophysics 437 (2), 691–697, 2005.

Smolkov, G.Ia., Pistolkors, A.A., Treskov, A.A., Krissinel, B.B., Putilov, V.A. The Siberian Solar Radio Telescope: parameters and principle of operation, objectives and results of first observations of spatio-temporal properties of development of active regions and flares. Astrophysics and Space Science 119 (1), 1–4, 1986.